A COMPOSITIONAL MODEL TO ASSESS EXPRESSION CHANGES FROM SINGLE-CELL RNA-SEQ DATA

By Xiuyu Ma[*], Keegan Korthauer[‡], Christina Kendziorski[†], and Michael Newton[*,†]

Department of Statistics[*], Department of Biostatistics and Medical Informatics[†], University of Wisconsin - Madison; Dana Farber[‡]

On the problem of scoring genes for evidence of changes in the distribution of single-cell expression, we introduce a empirical Bayesian mixture approach and evaluate its operating characteristics in a range of numerical experiments. The proposed approach leverages cell-subtype structure revealed in cluster analysis in order to boost gene-level information on expression changes. Cell clustering informs gene-level analysis through a specially-constructed prior distribution over pairs of multinomial probability vectors; this prior meshes with available model-based tools that score patterns of differential expression over multiple subtypes. We derive an explicit formula for the posterior probability that a gene has the same distribution in two cellular conditions, allowing for a gene-specific mixture over subtypes in each condition. Advantage is gained by the compositional structure of the model, in which a host of gene-specific mixture components are allowed, but also in which the mixing proportions are constrained at the whole cell level. This structure leads to a novel form of information sharing through which the cell-clustering results support gene-level scoring of differential distribution. The result, according to our numerical experiments, is improved sensitivity compared to several standard approaches for detecting distributional expression changes. **plus connection to bursting and other**

1. Introduction. The ability to measure genome-wide gene expression at single-cell resolution has accelerated the pace of biological discovery. Overcoming data analysis challenges caused by the scale and unique variation properties of single-cell data will surely fuel further advances in immunology (Papalexi and Satija, 2017), developmental biology (Marioni and Arendt, 2017), cancer (Navin, 2015), and other areas (Nawy, 2013). Computational tools and statistical methodologies created for data of lower-resolution (e.g., bulk RNA-seq) or lower dimension (e.g., flow cytometry) guide our response to the data science demands of new measurement platforms, but they remain inadequate for efficient knowledge discovery in this rapidly advancing domain (Bacher and Kendziorski, 2016).

An important feature of single-cell studies that could be leveraged better statistically is the fact that cells populate distinct, identifiable subtypes determined by lineage history, epigenetic state, the activity of various transcriptional programs, or other distinguishing factors. Extensive research on clustering cells has produced tools for identifying subtypes, including: SC3 (Kiselev et al., 2017), CIDR (Lin, Troup and Ho, 2017) and ZIFA (Pierson and Yau, 2015). We hypothesize that such subtype information may be usefully injected into other inference procedures in order to improve their operating characteristics.

Assessing the magnitude and statistical significance of changes in gene expression associated with changes in cellular condition has been a central statistical problem in genomics for which new tools specific to the single-cell RNAseq data structure have been deployed: MAST (Finak et al., 2015), SCDD (Korthauer et al., 2016), D3E (Delmans and Hemberg, 2016), etc. These tools respond to scRNAseq characteristics, such as high prevalance of zero counts and gene-level multimodality, but they do not fully exploit cellular-subtype information. We address this limitation, aiming to increase power to detect differential distribution. The proposed method measures changes in a gene's marginal mixture distribution, and acquires sensitivity to a wide variety of distributional effects by how it integrates genome-wide with gene-level data. It is implemented in software in the R package scDDBOOST, at http://github.com/wiscstatman/scDDboost/. Modularity in the necessary elements provides some methodological advantages. For example, improvements in clustering, such as *sc3?*, may be used in place of the default clustering, without altering the form of downstream analysis. **it's also relatively speedy computationally, not requiring any MCMC**

Through the compositional model underlying scDDboost, subtypes inferred by clustering inform the analysis of gene-level expression. The proposed methodology merges two lines of computation after cell clustering: one concerns patterns of differential expression among the cellular subtypes, and here we take advantage of the powerful EBseq method for detecting patterns in negative-binomially-distributed expression data (Leng et al., 2013). The second concerns the counts of cells in various subtypes; for this we propose a Double-Dirichlet-Mixture distribution to model the pair of multinomial probability vectors for subtype counts in two experimental conditions. Further elements are developed, on the selection of the number of subtypes and on accounting for uncertainty in the cluster output, in order to provide an end-to-end solution to the differential

distribution problem.

By way of example from stem-cell biology, Figure 1 shows data on several marker genes of G1 or G2/M phase that are called by `scDDboost` to be differentially distributed between two populations of cells (91 cells from G1 and 76 cells from G2/M). These particular genes were not detected by other standard approaches. Moreover, scDDboost identified in total 3395 DD genes, among them 409 genes are cell cycle annotated in Gene Ontology Cell Cycle biological process (GO:0007049) while other methods (MAST, scDD and DESeq2) in total identified 1970 genes with 228 genes are cell cycle related. (see Supplementary Material Section 1 for further details.)

The proposed method is often better able to detect weak changes compared to other methods, while at the same time agreeing with these methods on the strong differential signals and also not inflating the false-discovery rate.
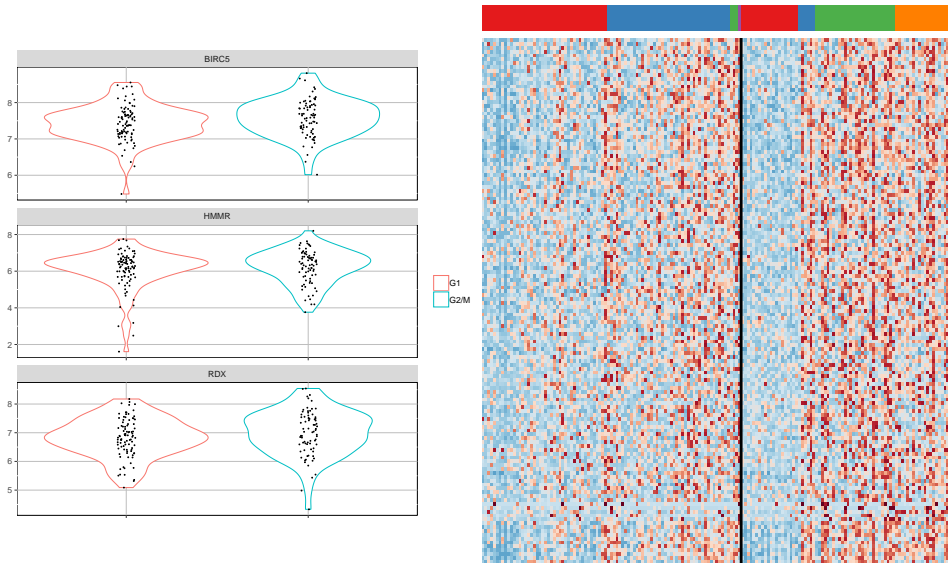

Fig 1: Cell cycle ralted genes uniquely identified by scDDboost from a study of stem cell differentiation (Leng *et al.* 2015). Shown are expression of 3 genes having functionality in cell cycles uniquely identified by scDDboost at 5% FDR. Right are heatmap for uniquely identified cell cycle related genes given by scDDboost BIRC5 is differentially expressed in the cell cycle (Li and Altieri, 1999),HMMR is differentially expressed in the cell cycle (Sohr and Engeland, 2008), RDX (not finalized version, needs to use other way to combine those two figs)

Numerical experiments on both synthetic and published scRNA-seq data indicate that `scDDboost` has high sensitivity for detecting subtle distribution changes. **link better with preceding paragraph* In these experiments we take advantage of `splatter` for generating synthetic data (Zappia, Phipson and Oshlack, 2017) as well as the compendium of scRNA-seq data available through `conquer` (Soneson and Robinson, 2017). **something on bursting?** We also establish first-order asymptotic results for the methodology. **any other results**

On organiziation, we present the modeling and methodology elements in Section 2, numerical experiments in Section 3, and a discussion in Section 4. For presentation we move some details to an appendix and many others to a Supplementary Material document.

2. Modeling.

2.1. *Data structure, sampling model, and parameters.* In modeling scRNASeq data, we imagine that each cell c falls into one of $K > 1$ classes, which we think of as subtypes or subpopulations of cells. For notation, $z_c = k$ means that cell c happens to be of subtype k, with the vector $z = (z_c)$ recording the states of all sampled cells. Knowledge of this class structure prior to measurement is not required, as it will be inferred as necessary from available genomic data. We expect that cells arise from multiple experimental conditions, such as by treatment-control status or some other factors measured at the cell level, but we present our development for the special case of two conditions. Notationally, $y = (y_c)$ records the experimental condition, say $y_c = 1$ or $y_c = 2$. Let's say condition j measures $n_j = \sum_c 1[y_c = j]$ cells, and in total we have $n = n_1 + n_2$ cells in the analysis. The examples in Section 3 involve hundreds to thousands of cells. Further let

$$(1) \qquad t_k^j = t_k^j(y, z) = \sum_c 1[y_c = j, z_c = k]$$

denote the number of cells of subtype k in condition j; we infer something about these counts using genome-wide data. As for molecular data, the normalized expression of gene g in cell c, say $X_{g,c}$, is one entry in a typically large GENES by CELLS data matrix X. Thus, the data structure entails an expression matrix X, a treatment label vector y, and a vector z of latent subtype labels.

We treat subtype counts in the two conditions, $t^1 = (t_1^1, t_2^1, \cdots, t_K^1)$ and $t^2 = (t_1^2, t_2^2, \cdots, t_K^2)$, as independent multinomial vectors, reflecting the

experimental design. Explicitly,

(2) $t^1|y \sim \text{Multinomial}_K(n_1, \phi)$ and $t^2|y \sim \text{Multinomial}_K(n_2, \psi)$

for probability vectors $\phi = (\phi_1, \phi_2, \cdots, \phi_K)$ and $\psi = (\psi_1, \psi_2, \cdots, \psi_K)$ that characterize the populations of cells from which the n observed cells are sampled. This follows from the more basic sampling model: $P(z_c = k|y_c = 1) = \phi_k$ and $P(z_c = k|y_c = 2) = \psi_k$.

Our working hypothesis, referred to as the *compositional model*, is that any differences in the distribution of expression $X_{g,c}$ between $y_c = 1$ and $y_c = 2$ (i.e., any condition effects) are attributable to differences between the conditions in the underlying composition of cell types; i.e., owing to $\phi \neq \psi$. We reckon that cells of any given subtype k will present data according to a distribution reflecting technical and biological variation specific to that class of cells, regardless of the condition the cell finds itself in. Some care is needed in this, as an overly broad cell subtype (e.g., *epithelial cells*) could have further subtypes that show differential response to some treatment, for example, and so cellular condition (treatment) would then affect the distribution of expression data within the subtype, which is contrary to our working hypothesis. Were that the case, we could have refined the subtype definition to allow a greater number of population classes K in order to mitigate the problem of within-subtype heterogeneity. A risk in this approach is that K could approach n, as if every cell were its own subtype. We find, however, that data sets often encountered do not display this theoretical phenomenon when considering a broad class of within-subtype expression distributions. We revisit the issue in Section 4, but for now we proceed assuming that cellular condition affects the composition of subtypes but not the distribution of expression within a subtype.

Within the compositional model, let $f_{g,k}$ denote the sampling distribution of expression measurement $X_{g,c}$ assuming that cell c is from subtype k. Then for the two cellular conditions, and at some expression level x, the marginal distributions over subtypes are finite mixtures:

$$f_g^1(x) = \sum_{k=1}^{K} \phi_k f_{g,k}(x) \quad \text{and} \quad f_g^2(x) = \sum_{k=1}^{K} \psi_k f_{g,k}(x).$$

In other words, $X_{g,c}|[y_c = j] \sim f_g^j$ and $X_{g,c}|[z_c = k, y_c = j] \sim f_{g,k}$.

We say that gene g is *differentially distributed*, denote DD_g and indicated $f_g^1 \neq f_g^2$, if $f_g^1(x) \neq f_g^2(x)$ for some x, and otherwise it is equivalently distributed (ED_g). Motivated by findings from bulk RNAseq data analysis, we

further set each $f_{g,k}$ to have a a negative-binomial form, say with mean $\mu_{g,k}$ and shape parameter σ_g; e.g. Leng et al. (2013), Anders and Huber (2010), and Love, Huber and Anders (2014). This choice is effective in our numerical experiments though it is not critical to the modeling formulation. The use of mixtures per gene has proven useful in related model-based approaches (e.g., Finak *et al.* 2015; McDavid *et al.* 2016; Huang *et al.* 2018). Our perspective is that genome-wide data may usefully inform the mixing proportions.

We seek methodology to prioritize genes for evidence of DD_g. Interestingly, even if we have evidence for condition effects on the subtype frequencies, it does not follow that a given gene will have $f_g^1 \neq f_g^2$; that depends on whether or not the subtypes show the right pattern of *differential expression* at g, to use the standard terminology from bulk RNAseq. For example, if two subtypes have different frequencies between the two conditions ($\phi_1 \neq \psi_1$ and $\phi_2 \neq \psi_2$) but the same aggregate frequency ($\phi_1 + \phi_2 = \psi_1 + \psi_2$), and also if $\mu_{g,1} = \mu_{g,2}$ then, other things being equal, $f_g^1 = f_g^2$ even though $\phi \neq \psi$. The fact is so central that we emphasize:

Key issue: A gene that does not distinguish two subtypes will also not distinguish the cellular conditions if those subtypes appear in the same aggregate frequency in the two conditions, regardless of changes in the individual subtype frequencies.

We formalize this issue in order that our methodology has the necessary functionality. To do so, first consider the parameter space $\Theta = \{\theta = (\phi, \psi, \mu, \sigma)\}$, where $\phi = (\phi_1, \phi_2, \cdots, \phi_K)$ and $\psi = (\psi_1, \psi_2, \cdots, \psi_K)$ are as before, where $\mu = \{\mu_{g,k}\}$ holds all the subtype-and-gene-specific expected values, and where $\sigma = \{\sigma_g\}$ holds all the gene-specific negative-binomial shape parameters. Critical to our construction are special subsets of Θ corresponding to partitions of the K cell subtypes. A single partition, say π, is a set of mutually exclusive and exhaustive blocks, b, say, each a subset of $\{1, 2, \cdots, K\}$, and we write $\pi = \{b\}$. Of course, the set Π containing all partitions π of $\{1, 2, \cdots, K\}$ has cardinality that grows rapidly with K. We carry along an example involving $K = 7$ cell types, and one three-block partition taken from the set of 877 possible partitions of $\{1, 2, \cdots, 7\}$ (Figure 1).

For any partition $\pi = \{b\}$, consider aggregate subtype frequencies

$$\Phi_b = \sum_{k \in b} \phi_k \quad \text{and} \quad \Psi_b = \sum_{k \in b} \psi_k,$$

and extend the notation, allowing vectors $\Phi_\pi = \{\Phi_b : b \in \pi\}$ and similarly

Fig 2: Proportions of $K = 7$ cellular subtypes in different conditions. Aggregated proportions of subtypes 3 and 4, subtypes 2, 5, and 6, and subtypes 1, and 7 remain same across conditions, while individual subtype frequencies change. Depending on the changes in average expression among subtypes, these frequency changes may or may not induce changes between two conditions in the marginal distribution of some gene's expression.

for Ψ_π. Recall the partial ordering of partitions based on refinement, and note that as long as π is not the most refined partition (every cell type its own block), then the mapping from (ϕ, ψ) to (Φ_π, Ψ_π) is many-to-one. Further, define sets

$$(3) \qquad\qquad A_\pi = \{\theta \in \Theta : \ \Phi_b = \Psi_b \,\forall b \in \pi\}.$$

and

$$(4) \qquad M_{g,\pi} = \{\theta \in \Theta : \ \mu_{g,k} = \mu_{g,k'} \iff k, k' \in b, b \in \pi\}.$$

Under A_π there are constraints on cell subtype frequencies; under $M_{g,\pi}$ there is equivalence in the gene-level distribution of expression between certain subtypes. These sets are precisely the structures needed to address differential distribution DD_g (and it complement, equivalent distribution, ED_g) at a given gene g, since:

 THEOREM 1. *Let $C_{g,\pi} = A_\pi \cap M_{g,\pi}$. For partitions $\pi_1 \neq \pi_2$, $C_{g,\pi_1} \cap C_{g,\pi_2} = \emptyset$. Further, at any gene g, equivalent distribution is*

$$\text{ED}_g = \bigcup_{\pi \in \Pi} C_{g,\pi}.$$

With additional probability structure on the parameter space, we immediately obtain from Theorem 1 a formula for local false discovery rates:

$$(5) \qquad 1 - P(\mathrm{DD}_g|X,y) = P(\mathrm{ED}_g|X,y) = \sum_{\pi \in \Pi} P\left(A_\pi \cap M_{g,\pi}|X,y\right).$$

Such local false discovery rates are important empirical Bayesian statistics in large-scale testing (e.g., Efron, 2007; Muralidharan, 2010; Newton *et al.* 2004). For example, the conditional false discovery rate of a list of genes is the arithmetic mean of the associated local false discovery rates. The partition representation guides construction of a prior distribution (Section 2.3) and a model-based method (Section 2.2) for scoring differential distribution. Setting the stage, Figure 2 shows the dependency structure of the proposed compositional model and the partition-reliant prior specification.

Fig 3: Directed acyclic graph structure of compositional model and partition-reliant prior. The plate on the right side indicates i.i.d. copies over cells c, conditionally on mixing proportions and mixing components. Observed data are indicated in rectangles/squares, and unobserved variables are in circles/ovals.

Key to computing the gene-specific local false discovery rate $P(\mathrm{ED}_g|X,y)$ is evaluating probabilities $P\left(A_\pi \cap M_{g,\pi}|X,y\right)$ for any subtype partition π and gene g. The dependence structure (Figure 2) implies a useful reduction of this quantity, at least conditionally upon subtype labels $z = (z_c)$.

THEOREM 2. $P\left(A_\pi \cap M_{g,\pi}|X,y,z\right) = P\left(A_\pi|y,z\right) P\left(M_{g,\pi}|X,z\right).$

In what follows, we develop the modeling and computational elements necessary to efficiently evaluate inference summaries (5) taking advantage of Theorems 1 and 2. Roughly, the methodological idea is that subtype labels z have relatively low uncertainty, and may be estimated from genome-wide clustering of cells in the absence of condition information y (up to an arbitrary label permutation). The modest bit of uncertainty in z we handle through a computationally efficient randomized clustering scheme. Theorem 2 indicates that our computational task then separates into two parts given z. On one hand, cell subtype frequencies combine with condition labels to give $P\left(A_\pi|y,z\right)$. Then gene-level data locally drive the posterior probabilities $P\left(M_{g,\pi}|X,z\right)$ that measure differential expression between subtypes. Essentially, the model provides a specific form of information sharing between genes that leverages the compositional structure of single-cell data in order to sharpen our assessments of between-condition expression changes.

2.2. *Method structure and clustering.* We leverage the extensive research on how to cluster cells into subtypes using scRNA-seq data: for example, SC3 (Kiselev et al., 2017), CIDR (Lin, Troup and Ho, 2017), and ZIFA (Pierson and Yau, 2015). We propose clustering on the full set of profiles in a way that is blind to the condition label vector y, in order to have as many cells as possible to inform the subtype structure. We investigated several clustering schemes in numerical experiments and allow flexibility in this choice within the scDDʙoost software. Associating clusters with subtype labels $\hat{z}_c$ estimates the actual subtypes z_c, and prepares us to use Theorems 1 and 2 in order to compute separate posterior probabilities $P(A_\pi|y,\hat{z})$ and $P(M_{g,\pi}|X,\hat{z})$ that are necessary for scoring differential distribution. The first probability concerns patterns of cell counts over subtypes in the two conditions, and has a convenient closed form within the double-Dirichlet model (Section 2.3). The second probability concerns patterns of changes in expected expression levels among subtypes, and this is also conveniently computed for negative-binomial counts using EBSᴇǫ (Leng et al., 2013). Algorithm 1 summarizes how these elements combine to get the posterior probability of differential distribution per gene, conditional on an estimate of the subtype labels.

We invoke $K-$medoids (Kaufman and Rousseeuw, 1987) as the default clustering method in scDDʙoost, and customize the cell-cell distance by integrating two measures. The first assembles gene-level information by cluster-based-similarity partitioning (Strehl and Ghosh, 2003). Separately at each gene, modal clustering (Dahl (2009) and Appendix B) partitions

---

Algorithm 1 scDDBoost-core

    Input:

        genes by cells expression data matrix $X = (X_{g,c})$

        cell condition labels $y = (y_c)$

        cell subtype labels (estimated) $\hat{z} = (\hat{z}_c)$

    Output: posterior probabilities of differential distribution from estimated subtypes

1: **procedure** scDDBoost-core$(X, y, \hat{z})$
2:   number of cell subtypes $K = \text{length}(\text{unique}(\hat{z}))$
3:     subtype differential expression: $\forall g, \pi$ compute $P(M_{g,\pi}|X, \hat{z})$ using `EBSeq`
4:     cell frequency changes: $\forall \pi$ compute $P(A_\pi|y, \hat{z})$ using Double Dirichlet model
5:     posterior probability: $\forall g, P(\text{ED}_g|X, y, \hat{z}) \leftarrow \sum_\pi P(M_{g,\pi}|X, \hat{z}) P(A_\pi|y, \hat{z})$
6:     **return** $\forall g, P(\text{DD}_g|X, y, \hat{z}) = 1 - P(\text{ED}_g|X, y, \hat{z})$
7: **end procedure**

---

the cells, and then we define dissimilarity between cells as the mahattan distance of those gene specific partition labels. A second measure defines dissimilarity by one minus the Pearson correlation between cells, which is computationally inexpensive, less sensitive to outliers than Euclidean distance, and effective at detecting cellular clusters in scRNA-seq (Kim et al., 2018). We combine the two measures by a weighted average, with $w_C = \frac{\sigma_P}{\sigma_C + \sigma_P}$ and $w_P = 1 - w_C$. where $w_C, \sigma_C, w_P, \sigma_P$ are the weights and standard deviations of cluster-based distance and Pearson-correlation distance, respectively. The final distance matrix is denoted $D = (d_{i,j})$.

Any clustering method entails classification errors, and so $\hat{z}_c \neq z_c$ for some cells. To mitigate the effects of this uncertainty, scDDBoost averages output probabilities from scDDBoost-core over randomized clusterings $\hat{z}^*$. These are not uniformly random, but rather are generated by applying $K-$medoids to a randomized distance matrix $D^* = (d_{i,j} \times w_{i,j})$, where $w_{i,j}$ are unit mean, non-negative weights $w_{i,j} = 1/(e_i + e_j)$, and where (e_i) are independent and identically Gamma$(\hat{a}, \hat{b})$ distributed deviates for hyper-parameters $(\hat{a}, \hat{b})$ derived from D. We argue that the distribution of clusterings induced by this simple computational scheme approximates a Bayesian posterior analysis (Supplementary Material Section **). Pseudo-code for the resulting scDDBoost is in Algorithm 2 (Appendix). Averaging this way gives additional stability to the posterior probability statistics (Supplementary Material Section **).

Computations become more intensive the larger is the number K of cell subtypes. We also observe that taking K to be too large may inflate the false positive rate (Figure **). The approach taken in `scDDboost` is to set K using

the validity score (Ray and Turi, 2000), which measures changes in within-cluster sum of squares as we increase K. Our specific implementation is in Supplementary Material Section *.

2.3. *Double Dirichlet Mixture (DDM).* Here we describe the partition-reliant prior $p(\phi, \psi)$ indicated in Figure 2 and derive an explicit formula for $P(A_\pi | y, z)$. We lose no generality here by defining $A_\pi = \{(\phi, \psi) : \Phi_b = \Psi_b \ \forall b \in \pi\}$, rather than as a subset of the full parameter space as in (3). Each A_π is closed and convex subset of the product space holding all possible pairs of length-K probability vectors.

We propose a spike-slab-style mixture prior with the following form:

(6)
$$p(\phi, \psi) = \sum_{\pi \in \Pi} \omega_\pi \, p_\pi(\phi, \psi).$$

Each mixture component $p_\pi(\phi, \psi)$ has support A_π; the mixing proportions ω_π are any non-negative constants summing to one. To specify component p_π, notice that on A_π there is a 1-1 correspondence between pairs (ϕ, ψ) and parameter states:

(7)
$$\{(\tilde{\phi}_b, \tilde{\psi}_b, \Phi_b), \ \forall b \in \pi\},$$

where

$$\tilde{\phi}_b = \frac{\phi_b}{\Phi_b}, \quad \tilde{\psi}_b = \frac{\psi_b}{\Psi_b}, \quad \text{and} \quad \Phi_b = \sum_{k \in b} \phi_k = \sum_{k \in b} \psi_k = \Psi_b.$$

For example, $\tilde{\phi}_b$ is a vector of conditional probabilities for each subtype given that a cell from the first condition is one of the subtypes in b.

We introduce hyperparameters $\alpha_k^1, \alpha_k^2 > 0$ for each subtype k, and set $\beta_b = \sum_{k \in b} (\alpha_k^1 + \alpha_k^2)$ for any possible block b. Extending notation, let α_b^j be the vector of α_k^j for $k \in b$, β_π be the vector of β_b for $b \in \pi$, ϕ_b and ψ_b be vectors of ϕ_k and ψ_k, respectively, for $k \in b$, and Φ_π and Ψ_π be the vectors of Φ_b and Ψ_b for $b \in \pi$. The proposed double-Dirichlet component p_π is determined in the transformed scale by assuming $\Psi_\pi = \Phi_\pi$ and further:

(8)
$$\begin{aligned}
\Phi_\pi &\sim \text{Dirichet}_{N(\pi)}[\beta_\pi] \\
\tilde{\phi}_b &\sim \text{Dirichlet}_{N(b)}[\alpha_b^1] \qquad \forall b \in \pi \\
\tilde{\psi}_b &\sim \text{Dirichlet}_{N(b)}[\alpha_b^2] \qquad \forall b \in \pi
\end{aligned}$$

where $N(\pi)$ is the number of blocks in π and $N(b)$ is the number of subtypes in b, and where all random vectors in (8) are mutually independent. Mixing over π as in (6), we write $(\phi, \psi) \sim \text{DDM}\left[\omega = (\omega_\pi), \alpha^1 = (\alpha_k^1), \alpha^2 = (\alpha_k^2)\right]$.

We record some properties of the component distributions p_π:

Property 1: In $p_\pi(\phi, \psi)$, ψ and ϕ are dependent, unless π is the null partition in which all subtypes constitute a single block.

Property 2: With $k \in b$, marginal means are:

$$E_\pi(\phi_k) = \frac{\alpha_k^1}{\sum_{k' \in b} \alpha_{k'}^1} \frac{\beta_b}{\sum_{b' \in \pi} \beta_{b'}} \quad \text{and} \quad E_\pi(\psi_k) = \frac{\alpha_k^2}{\sum_{k' \in b} \alpha_{k'}^2} \frac{\beta_b}{\sum_{b' \in \pi} \beta_{b'}}.$$

Recall from (1) the vectors t^1 and t^2 holding counts of cells in each subtype in each condition, computed from y and z. Relative to a block $b \in \pi$, let $t_b^j = \sum_{k \in b} t_k^j$, for cell conditions $j = 1, 2$, and, let t_π^j be the vector of these counts over $b \in \pi$. The following properties refer to marginal distributions in which (ϕ, ψ) have been integrated out of the joint distribution involving (2) and the component p_π.

Property 3: t^1 and t^2 are conditionally independent given y, t_π^1 and t_π^2.

Property 4: For $j = 1, 2$,

$$p_\pi(t^j | t_\pi^j, y) = \prod_{b \in \pi} \left\{ \left[\frac{\Gamma(t_b^j + 1)}{\prod_{k \in b} \Gamma(t_k^j + 1)} \right] \left[\frac{\Gamma(\sum_{k \in b} \alpha_k^j)}{\prod_{k \in b} \Gamma(\alpha_k^j)} \right] \left[\frac{\prod_{k \in b} \Gamma(\alpha_k^j + t_k^j)}{\Gamma(t_b^j + \sum_{k \in b} \alpha_k^j))} \right] \right\}$$

Property 5:

$$p_\pi(t_\pi^1, t_\pi^2 | y) = \left[\frac{\Gamma(n_1 + 1)\Gamma(n_2 + 1)}{\prod_{b \in \pi} \Gamma(t_b^1 + 1)\Gamma(t_b^2 + 1)} \right] \left[\frac{\Gamma(\sum_{b \in \pi} \beta_b)}{\prod_{b \in \pi} \Gamma(\beta_b)} \right] \left[\frac{\prod_{b \in \pi} \Gamma(\beta_b + t_b^1 + t_b^2)}{\Gamma(n_1 + n_2 + \sum_{b \in \pi} \beta_b)} \right].$$

Let's look at some special cases to dissect this result.

Case 1. If π has a single block equal to the entire set of cell types $\{1, 2, \cdots, K\}$, then $t_b^j = n_j$ for both $j = 1, 2$, and Property 5 reduces, correctly, to $p_\pi(t_\pi^1, t_\pi^2 | y) = 1$. Further,

$$p_\pi(t^j | t_\pi^j, y) = \left[\frac{\Gamma(n_j + 1)}{\Gamma(n_j + \sum_{k=1}^K \alpha_k^j)} \right] \left[\frac{\Gamma(\sum_{k=1}^K \alpha_k^j)}{\prod_{k=1}^K \Gamma(\alpha_k^j)} \right] \left[\prod_{k=1}^K \frac{\Gamma(\alpha_k^j + t_k^j)}{\Gamma(t_k^j + 1)} \right]$$

which is the well-known Dirichlet-multinomial predictive distribution for counts t^j (Wagner and Taudes, 1986). E.g, taking $\alpha_k^j = 1$ for all types k we get the uniform distribution

$$p_\pi(t^j | t_\pi^j, y) = \frac{\Gamma(n_j + 1)\Gamma(K)}{\Gamma(n_j + K)}.$$

Case 2. At the opposite extreme, π has one block b for each class k, so $\phi = \psi$. Then $p_\pi(t^j|t^j_\pi, y) = 1$, and further, writing $b = k$,

$$p_\pi(t^1_\pi, t^2_\pi|y) = \left[\frac{\Gamma(n_1 + 1)\Gamma(n_2 + 1)}{\prod_{k=1}^{K} \Gamma(t^1_k + 1)\Gamma(t^2_k + 1)} \right] \left[\frac{\Gamma(\sum_{k=1}^{K} \beta_k)}{\prod_{k=1}^{K} \Gamma(\beta_k)} \right] \left[\frac{\prod_{k=1}^{K} \Gamma(\beta_k + t^1_k + t^2_k)}{\Gamma(n_1 + n_2 + \beta_k)} \right].$$

which corresponds to Dirichlet-multinomial predictive distribution for counts $t^1 + t^2$ since t^1 and t^2 are identical distributed given (ϕ, ψ) in this case.

The properties above are useful in establishing:

THEOREM 3. *The DDM model is conjugate to multinomial sampling of t^1 and t^2:*

$$(\phi, \psi)|y, z \sim \text{DDM}\left[\omega^{\text{post}} = (\omega^{\text{post}}_\pi), \alpha^1 + t^1, \alpha^2 + t^2\right]$$

where

$$\omega^{\text{post}}_\pi \propto p_\pi(t^1|t^1_\pi, y)\, p_\pi(t^2|t^2_\pi, y)\, p_\pi(t^1_\pi, t^2_\pi|y)\, \omega_\pi.$$

The target probability $P(A_\pi|y, z)$ is an integral of the posterior distribution in Theorem 3. To evaluate it, we need to contend with the fact that sets $\{A_\pi : \pi \in \Pi\}$ are not disjoint. Relevant overlaps have to do with partition refinement. Recall that a partition π^r is a refinement of a partition π^c if $\forall b \in \pi^c$ there exists $s \subset \pi^r$ such that $\underset{b' \in s}{\cup} b' = b$. We say π^c coarsens π^r when π^r refines π^c. Any partition both refines and coarsens itself, as a trivial case. Generally, refinements increase the number of blocks. If subtype frequency vectors (ϕ, ψ) satisfy the constraints in A_{π^r} then they also satisfy the constraints of any π^c that coarsens π^r: i.e., $A_{\pi^r} \subset A_{\pi^c}$. Refinements reduce the dimension of allowable parameter states. For the double-Dirichlet component distributions P_π, we find:

Property 8: For two partitions $\tilde{\pi}$ and π,

$$P_{\tilde{\pi}}(A_\pi|y, z) = \begin{cases} 1 & \text{if } \tilde{\pi} \text{ refines } \pi \\ 0 & \text{otherwise} \end{cases}$$

This supports the main finding of this section:

$$(9) \qquad P(A_\pi|y, z) = \sum_{\tilde{\pi} \in \Pi} \omega^{\text{post}}_{\tilde{\pi}} 1[\tilde{\pi} \text{ refines } \pi].$$

3. Numerical experiments.

3.1. *Synthetic data.* To assess the performance of `scDDboost` we first simulated synthetic data using `splatter` (Zappia, Phipson and Oshlack, 2017), a recently developed system having good empirical characteristics and providing interface for simulating cells from multiple groups. We assess the performance of scDDboost on identifying DD genes and comparing the power to other three methods scDD, MAST and DESeq2. Splatter provides two user specified parameters: location θ and scale γ for controlling how different the transcripts of a gene can be between groups. For simplicity of writing, we refer the pair of those two parameters as DE parameters. In the paper, the author used $\theta = -0.1$ and $\gamma = 0.3$, in the R package, the default value is $\theta = 0.1$ and $\gamma = 0.4$. However, all of our candidate methods have low true positive rate under the default settings(Fig4) as the differences between groups are small. This is consistent with the phenomena reported in the splatter paper. To better evaluate those methods, we use another two configurations of $(\theta = -0.1, \gamma = 1)$ and $(\theta = 0.3, \gamma = 0.5)$, which zoom in the heterogeneities between subtypes and keep the parameters close to default ones thus the identification of subtypes and DD analysis still remain chanllenging. Supplementary S1) Other nuisance parameters are set to default values.

We simulate datasets under 3 different number of groups : $K = 3, 7, 12$. As feasibility of computation, scDDboost can only handle K up to 9. We assess whether scDDboost can still be powerful when underestimating the number of subtypes. For the

Considering the above 4 choices of DE parameters and 3 choices of K, we have in total 12 simulation scenarios and each scenario we have 2 replicates.

We compare the true positive rate and false discovery rate (results are averaged over replicates) between the four methods(Fig 4 and 5) We found that scDDboost identified most true DD genes meanwhile having the lowest FDR. The reason is that genes transcripts are distributed more homogeneously within the same cluster than between clusters. Grouping cells first enable us to detect the subtle change of expression level between clusters, which may cause the marginally change not significant enough to be detected by other scRNA methods like MAST and DESeq2. scDD considered mixture structure underlying the transcrips as well, but scDD did not use the whole genome information to infer mixture components, which leads to inaccurate clustering at gene level and reduce the power.
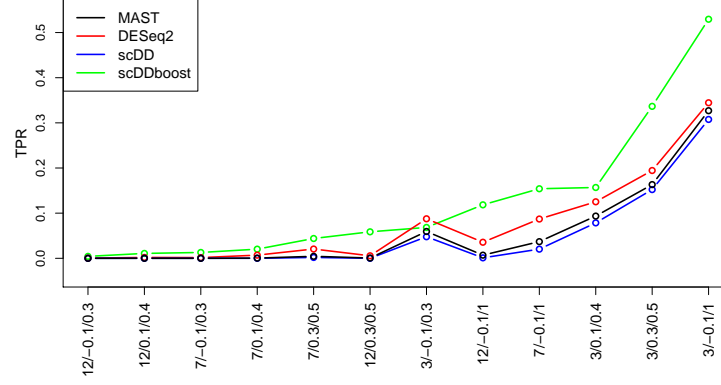
Fig 4: True positive rate averaged over replicates of four methods under 3 settings of number of subtypes and 4 hyper parameters govern the difference between subtypes, threshold = 0.05, ordered by true positive rate of scDDboost names are in the format K / shape / scale
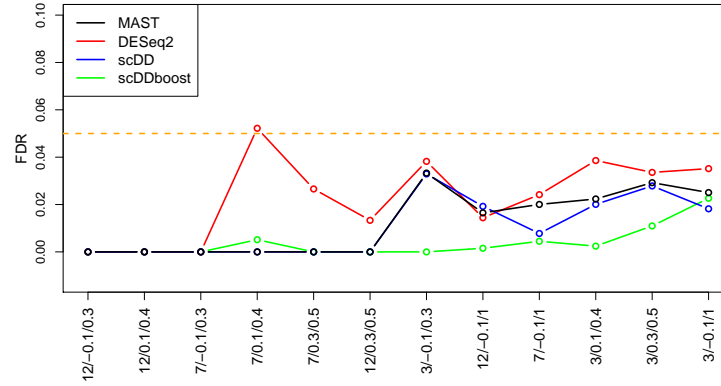

Fig 5: FDR averaged over replicates of four methods under 3 settings of number of subtypes and 4 hyper parameters govern the difference between subtypes, threshold = 0.05,ordered by true positive rate of scDDboost same order as Fig 4

3.2. *Empirical study.* We use 12 data sets from previously published papers and `conquer` (Soneson and Robinson, 2017) to test performance of our method on empirical data.(datasets information are in the supplementary material) Among those 12 datasets. 11 of them each condition having

$50 \sim 200$ cells and the other one (GSE84465) having larger number of cells with 1300 cells in condition 1 and 700 cells in condition 2. We generally assess the power of scDDboost by comparing the number of DD genes identified by different methods. GSE64016(Fucci) dataset are used for further evaluation and validate that our method did uniquely identify some genes biologically meaningful.

We have also investigated performance of `scDDboost` under different clustering method, (`sc3` (Kiselev et al., 2017), Supplementary ***) and obtain similar results as the default one.
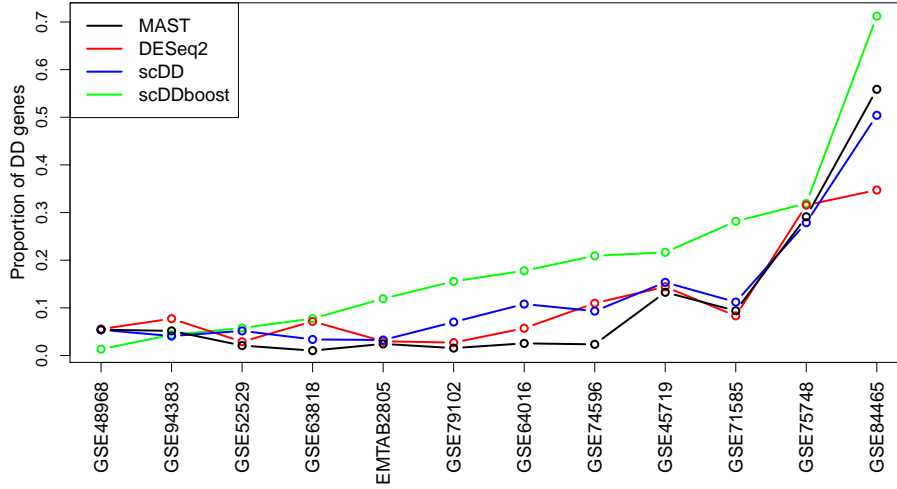

Fig 6: Proportion of DD genes at 5% threshold with respect to total number of genes identified by each method. Ranked by mean list size

We observe that scDDboost generally identify more DD genes than other methods.

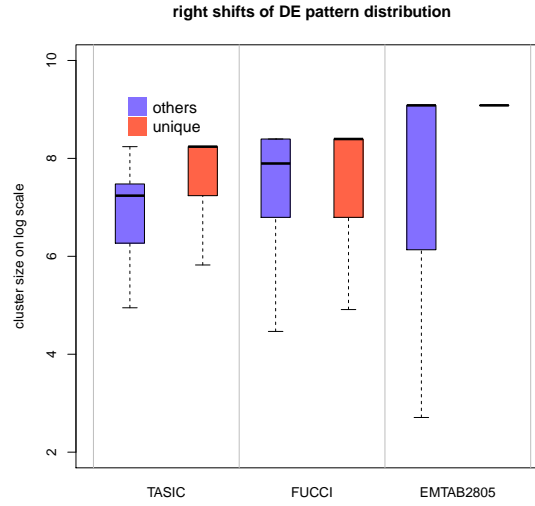***Benefits from share information from other genes in EBSeq. ***

Fig 7: boxplot of log transformed cluster size of DD genes of two categories. The red one are corresponding to the genes that have also been identified by other methods. The blue one are corresponding to the genes uniquely identified by scDDboost. We grouped genes to the same cluster if they share the same map DE pattern between subtypes inferred from EBSeq We use the number of genes within a cluster as the size for that cluster. We observe a right shift for between blue and right, which indicates our uniquely identified DD genes are more likely to associate with DE patterns of larger sizes Datasets used for demonstration from left to right are GSE71585, GSE64016, EMTAB2805. Here we used 0.01 threshold as it is more friendly for graphical demostration, 0.05 cases are in the supplementary fig *** (still have right shift, but hard to see from box plot as most of genes are associated with the largest cluster, the right shift did not change the quantile too much)

3.3. *Null cases.* Although bulk methods seems to be the most powerful one, we found it also has a higher false discovery rate comparing to single cell methods. We validate false discovery rate on ten null datasets from table 1. For each null dataset, we randomly split the cells from one condition into two subsets and test difference of gene expression between those subsets. Since the two subsets of cells actually came from same condition, there should not be any differential distributed genes, any positive call would be a false positive. We repeat the random split and testing for five times on each null data set. We evaluate the type I error control for the methods returning nominal p-values, by recording the fraction of genes(with a valid p-value) that are assigned a nomial p-value below 0.05 (Fig 6).

scDDboost could control FDR since we assume cells are sampled from

population composed of different subtypes. Cells from one subtype are equal likely to be assigned to either one of the two subsets. Consequently, it is very likely that proportions of subtypes remain unchanged among the two subsets.
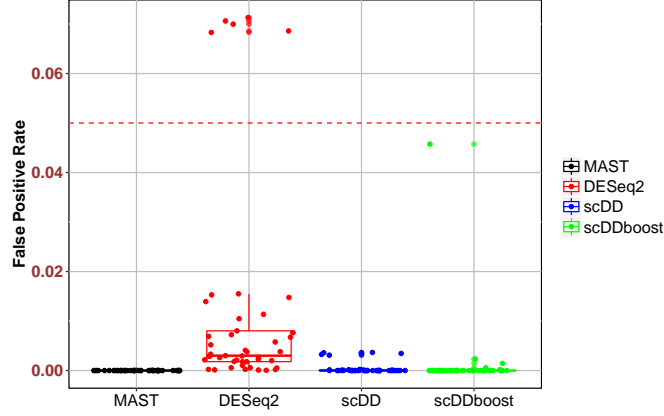

Fig 8: False positive rate of scDDboost, scDD, MAST and DESeq2 on null dataset from table 1, DESeq2 usually identify a lot but may lose the control of type I error. While other single cell methods could control FDR.

Number of subtypes K is a crucial factor controlling the accuracy of our modeling. Too small K may end up in an underfit such that cells within same subtype can still be very different, such heterogeneity within the subtype introduced by insufficient number of clusters tends to make our posterior inference of the DE patterns between subtypes more favorable for all equivalent expressed and reducing the power of scDDʙᴏᴏsᴛ. Too big K may end up in an overfit such that two subtypes can be very similar, given we have fixed number of samples (cells), allowing more clusters will introduce more patterns (both for mean expression change and proportion change) to infer. Also notice the limitation of DDM model (see section 4), overestimating K in scDDʙᴏᴏsᴛ may losing FDR control (supplementary Fig number ***).

3.4. *Bursting.* ***on the method estimated p-value, update later***

D3E(Delmans and Hemberg, 2016) is a distributional method that can identify bursting parameters of transcripts. Rate of promoter activation, rate of promoter inactivation and the rate of transcription when the promoter is in the active state are estimated by D3E. We investigate DD genes identified by scDDboost and their change of those three parameters on
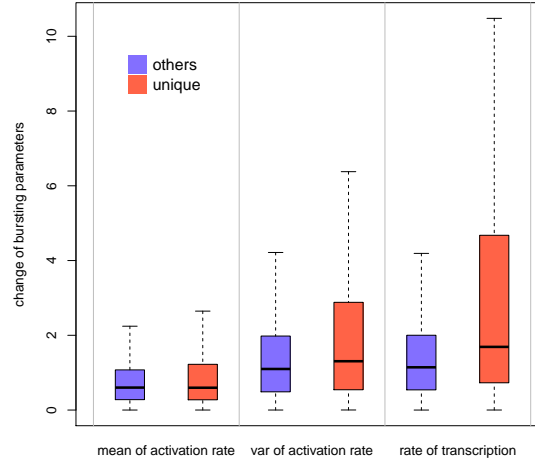
dataset GSE71585

Fig 9: Absolute value of log fold change of bursting parameters estimated by D3E methods across conditions (DEC vs EC). Purple box refers to those DD genes identified by other methods, magenta box refers to DD genes uniquely identified by scDDboost. In the D3E model, it assumes the counts are sampled from a poisson-beta model. Specifically, $x \sim$ $\text{Poi}(x|\gamma * p)$, $p \sim \text{Beta}(\alpha, \beta)$, In D3E paper, it call α the rate of promoter activation, β the rate of promoter inactivation and γ the rate of transcripts when the promoter is in the active state. Such poisson-beta model should be the stationary distribution of the transcriptional bursting model. For each condition each gene D3E would estimate a triplet (α, β, γ). Instead of directly looking at the change of α, β. I looked at the change of mean and variance of Beta prior for each condition. i.e. the change for mean and var for p from the poisson-beta model. I think it would be more natural to look at p, as transcripts are more directly related to p than α and β, $p = 0$ would mean the promoter is off and $p = 1$ means the promoter is on, so p is more like a measure for how likely a promoter is on, I call the mean and var of p as the mean and var of activation rate. Then I plot the absolute value of log fold change of mean, var activation rate and rate of transcripts γ. Those uniquely identified genes by scDDboost are more consistent with the estimations from D3E since they are corresponding to more significant change of those bursting parameters

We observed that DD genes identified by scDDboost tends to have similar transcription rate when the promoter is active across condition, while there are lots of variabilities in the action and inactivation rate. Estimations from D3E reveals that the major factor to drive DD genes are activation and inactivation rate (proportions of different subtyps), it make sense to

consider mixture model like scDDboost.

4. Theoretical issues.

4.1. *Posterior consistency.* Under some parameters settings, the double dirichlet prior will have limited resolution and lead to inconsistency of posterior probabilities, which we investigate with the following asymptotic analysis.

We first give the expression of posterior probability. Since there is no information favorable of any particular A_π, we select discrete uniform distribution as the prior for it, then the posterior probability is

$$(10) \qquad p(A_\pi|t^1, t^2) = c * \sum_{\pi' \text{ refines } \pi} p(t^1|t^1_{\pi'})\, p(t^2|t^2_{\pi'})\, p(t^1_{\pi'}, t^2_{\pi'}|A_{\pi'})$$

for a normalizing constant $\frac{1}{c} = \sum_{\pi' \in \Pi} p(t^1|t^1_{\pi'})\, p(t^2|t^2_{\pi'})\, p(t^1_{\pi'}, t^2_{\pi'}|A_{\pi'})$.

Let $\Omega = \{(\phi, \psi) : \sum_{i=1}^{K} \phi_i = \sum_{i=1}^{K} \psi_i = 1, \phi_i \geq 0, \psi_i \geq 0, i = 1, ..., K\}$ be the whole space. There is a subset of Ω we lack posterior inference. Let us first see an example:
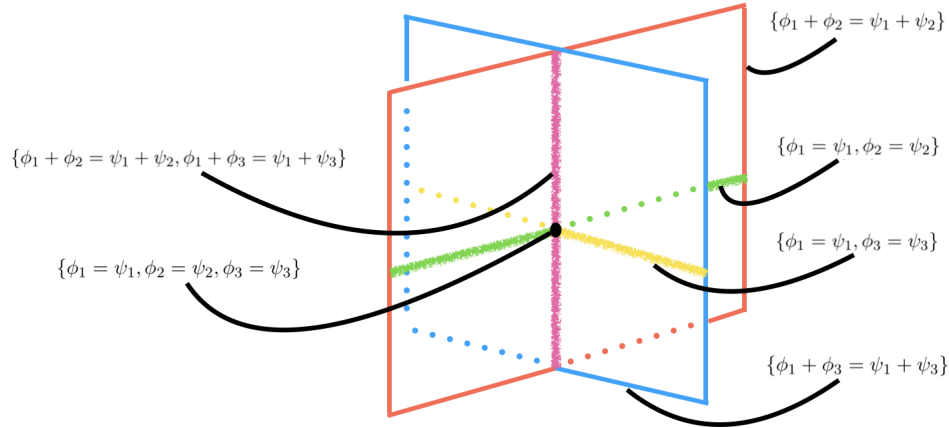

Fig 10: Four subtypes of cells, simplexes of (ϕ, ψ) satisfying different constraints.

In Fig 10, there are four subtypes, the rectangle with magenta boundary is a simplex $A_{\pi_1} = \{(\phi, \psi) : \phi_1 + \phi_2 = \psi_1 + \psi_2\}$, the rectangle with blue boundary is a simplex $A_{\pi_2} = \{(\phi, \psi) : \phi_1 + \phi_3 = \psi_1 + \psi_3\}$. The green line refers to $A_{\pi_3} = \{(\phi, \psi) : \phi_1 = \psi_1, \phi_2 = \psi_2\}$, the yellow line refers to $A_{\pi_4} = \{(\phi, \psi) : \phi_1 = \psi_1, \phi_3 = \psi_3\}$, the purple line refers to $A_{\pi_5} = \{(\phi, \psi) : \phi_1 + \phi_2 = \psi_1 + \psi_2, \phi_1 + \phi_3 = \psi_1 + \psi_3\}$, which is the intersection of A_{π_1} and A_{π_2}, and finally the black dot which is the intersection of those three lines refers to the simplex with finest partitions, $\phi_i = \psi_i, \forall i = 1, .., 4$. We lack posterior inference for (ϕ, ψ) along the purple line except the black dot. While on the green line, yellow line and black dot, we have consistent posterior inference(theorem 2). To explain why some space lacking posterior inference and define such space, we define a special subset A_π^* of simplex A_π. $A_\pi^* = A_\pi \setminus \bigcup_{\tilde{\pi} \text{ is not coarser than } \pi} A_{\tilde{\pi}}$, A_π^* is obtained by removing all intersection with other $A_{\tilde{\pi}}$(excluding those $A_{\tilde{\pi}}$ that is superset of A_π) from A_π. Since we removed those intersection parts. It is intuitive that A_π^* will be disjoint subsets of Ω.

PROPOSITION 1. *if* $\pi_1 \neq \pi_2$, *then* $A_{\pi_1}^* \cap A_{\pi_2}^* = \varnothing$

Let $Q = \Omega \setminus \bigcup_{\pi \in \Pi} A_\pi^*$, and we have following proposition of the existence of Q.

PROPOSITION 2. *Let K be number of subtypes. When $K > 3, Q \neq \varnothing$, when $K \leq 3, Q = \varnothing$*

When the number of subtypes is bigger than three, we lack posterior inference on Q. To see that we can rewrite A_π^* as $A_\pi^* = A_\pi \setminus \bigcup_{\tilde{\pi} \text{ is not coarser than } \pi} (A_{\tilde{\pi}} \cap A_\pi)$, $\tilde{\pi}$ is not coarser than π, which is equivalently to say π is not refinement of $\tilde{\pi}$. By property 8 in section 2, $A_{\tilde{\pi}} \cap A_\pi$ is a lower dimensional subset of A_π. So $A_\pi \setminus A_\pi^*$ is a lower dimensional subset of A_π. For posterior on Q, it degenerates to integral on a lower dimensional subset of the simplex associating with densities, which will vanish

PROPOSITION 3. *When $K > 3$, $p(Q|z^1, z^2) = 0$*

But for $(\phi, \psi) \in \Omega \setminus Q$, we have consistent posterior inference.

THEOREM 4. *Let $n = min(n_1, n_2)$ be the smaller number of cells of two conditions and $n_1 = O(n_2)$ namely $ln(\frac{n_1}{n_2}) = 0$, and hyper parameters of DDM α^1, α^2 be vectors of constants, $\alpha_k^j \geq 1, \forall k, j$ and $\beta = \alpha^1 + \alpha^2$. Then if parameter $(\phi, \psi) \in \Omega \setminus Q$ we have*

$$p(A_\pi | y, z) \xrightarrow[n \to \infty]{a.s.} \begin{cases} 1 & \text{if } (\phi, \psi) \in A_\pi \\ 0 & \text{otherwise} \end{cases}$$

Things become more complicate when (ϕ, ψ) falling into Q, we know $p(Q | y, z)$ vanishes, but $p(A_\pi | y, z)$ may not.

Recall $N(\pi)$ represents number of blocks b in π. Let $S = \{\pi, (\phi, \psi) \in A_\pi\}$, which is the collection of partitions whose associated simplexes covering (ϕ, ψ). Let $N^* = \max_{\pi \in S} N(\pi)$, which is the max number of blocks of partitions from S. Let $S^* = \{\pi, (\phi, \psi) \in A_\pi \text{ and } N(\pi) = N^*\}$, which is the collection of partitions that covering (ϕ, ψ) with number of blocks equal to the max number N^*.

For example, when $K = 7$, For a $(\phi, \psi) \in A_{\pi_1} \cap A_{\pi_2} \cap A_{\pi_3}$, $\pi_1 = \{\{1, 2, 3\}, \{4, 5, 6, 7\}\}, \pi_2 = \{\{1, 6, 7\}, \{2, 4\}, \{3, 5\}\}, \pi_3 = \{\{1, 2, 3, 4, 5, 6\}\}$, and also (ϕ, ψ) does not belong to any other simplex A_π. Then $S = \{\pi_1, \pi_2, \pi_3\}, N^* = 3, S^* = \{\pi_2\}$.

THEOREM 5. *Following the setting in theorem 4, when parameter $(\phi, \psi) \in Q$, and further if $\alpha^j, j = 1, 2$ are vectors of integers, we have*

$$(p(A_\pi | y, z))_{\pi \in S^*} \xrightarrow[n \to \infty]{d} (V_1, ..., V_{N(S^*)})$$

$V_1, ..., V_{N(S^*)}$ are random variables and $V_1 + .. + V_{N(S^*)} = 1$

Still using above example, in limiting case, we have $p(A_{\pi_3} | y, z) = 1$, $p(A_{\pi_2} | y, z) = 1$ and $p(A_{\pi_1} | y, z) = 0$. When the DE pattern is B_{π_1} for some genes and our estimation of $p(A_{\pi_1} | y, z) = 0$, we will falsely classify those genes as differential distributed.

The asymptotic properties help us gain insight of the performance of our approach, scDDboost may work poorly, when $(\phi, \psi) \in Q$, we may underestimate the posterior probability of true proportion change pattern,

which reduce the posterior probabilities of true negative and enlarge false positive rate.

4.2. *Random weighting.* In this section, we gave an intuitive justification for consistency between bayesian framework clustering analysis and random weighting procedure. A full bayesian analysis for clustering needs to specify the density of data given the partition. Specifically, in single cell analysis we need to know the density of transcripts of genes given the partitions which requires understanding of co-expression and dependence between genes. Instead of trying to untangle the mystery behind the dependence of genes, we consider following approximation

$$P(\text{Partition}|X) \leftarrow P(\text{Partition}|D) \leftarrow P(\Delta|D) \leftarrow D/W$$

where D is the estimated distance matrix of X, Δ is the true distance of X and W is randomly distributed matrix of weights. We conjecture that the probability of partitions given data can be approximated by switching conditioning on data to conditioning on the estimated distance of data. As distance matrix typically gave the geometrical structure between elements which can be used to infer how likely a partition is. In addition, partition can be obtained by distance based clustering algorithm (K-medoids) on true distance matrix Δ. To approximate distribution $(\Delta|D)$, we use our random weighting procedure, namely sampling a weighting matrix W first and then do the component-wisely dividing of original distance matrix D by W.

We gave a brief justification for this approximation, suppose units i and j are merged into a common cluster if (and only if) $d_{i,j} < c$. Then $P(d_{i,j}^* < c) = P(w_{i,j} > c/d_{i,j})$, $w_{i,j} \sim \text{Gamma}(a, a)$. From Bayesian perspective, given the true distance $\Delta_{i,j}$, $d_{i,j}|\Delta_{i,j} \sim \text{Gamma}(a_1, a_1/\Delta_{i,j})$, so that the sampling mean of $d_{i,j}$ is $\Delta_{i,j}$. Further, for simplicity we ignore any issues about the d's or Δ's being true distances. The condition for qualifiable distance matrix is the triangle inequality among the pairwise distances, such condition would not affect our clustering results too much. But, a simple analysis might suppose that a-priori $1/\Delta_{i,j} \sim \text{Gamma}(a_0, d_0)$. The scaling is such that $\text{E}(1/\Delta_{i,j}) = a_0/d_0$. The posterior, by conjugacy, has $1/\Delta_{i,j}|d_{i,j} \sim \text{Gamma}(a_0 + a_1, d_0 + a_1 d_{i,j})$. Then the posterior probability that i and j should be clustered is the posterior probability that $\Delta_{i,j} < c$, which is $P(\text{Gamma}((a_0 + a_1), (a_0 + a_1)) > (d_0 + a_1 * d_{i,j})/(a_0 + a_1) * 1/c)$.

In order to match the posterior probability that elements *i* and *j* belongs to the same cluster through the simple bayesian analysis to random weighting, we need d_0 to be small and $a = a_0 + a_1$. For the estimation, we fixed d_0 and estimating (a_0, a_1) from maximizing the marginal likelihood of $d_{i,j}$. Therefore, we gave a way of modeling the distribution of weights such that partition based on random generated distance D/W would approximate the partition given data based on a full bayesian framework.

5. Discussion. We have presented scDDboost, a compositional model for detecting differential distributed genes from scRNA-seq data. To account for the over-dispersion and multi-modality of single-cell data, scDDboost modeled transcripts as mixture distributed. Unlike previous invented methods (e.g. Deseq2, MAST and scDD), which conducts genewise DD test in an isolated manner. scDDboost make whole genome information shared at gene level by further assuming the mixture distribution of transcripts is a mixture over the subtypes of cells. Another advantage of scDDboost is its' flexibility to allow user specified clustering methods of cells, with more and more studies of the scRNA-seq data, there will be more accurate distance matrix between cells, which will yield better estimation of subtypes and inference of DD genes. We combine estimations of changes of subtypes' proportions across conditions and changes of mean expressions across subtypes to infer distributional changes of transcripts. To estimate changes of subtypes' proportions across conditions, we use empirical Bayes and developed a double Dirichlet prior distribution. We invented a random weighting scheme that stabilize our DD inference as well as approximating the results as if we have done a fully bayesian clustering analysis based on Dirichlet prior. We demonstrated that scDDboost outperforms existing approaches in simulation and tends to be more powerful than existing methods on a wide range of public available empirical datasets.

One limitation of scDDboost is that current EBseq inference of the DE patterns is computationally not feasible for big number of subtypes. Given the noise level among the single cell data and especially if we want to identify DD genes among conditions containing thousands of cells, allowing a big number of subtypes would make cells under same subtype more homogeneous and result in a more accurate estimations for the distribution of transcripts. Further research is needed for acceleration of EBseq, one direction is to reduce the calculation on those patterns that would have small posterior probabilities.

References.

ANDERS, S. and HUBER, W. (2010). Differential expression analysis for sequence count data. *Genome Biology* **11** R106–R106.

BACHER, R. and KENDZIORSKI, C. (2016). Design and computational analysis of single-cell RNA-sequencing experiments. *Genome Biology* **17** 63. .

DAHL, D. B. (2009). Modal clustering in a class of product partition models. *Bayesian Anal.* **4** 243–264.

DELMANS, M. and HEMBERG, M. (2016). Discrete distributional differential expression (D3E) - a tool for gene expression analysis of single-cell RNA-seq data. *BMC Bioinformatics* **17** 110. .

FINAK, G., MCDAVID, A., YAJIMA, M., DENG, J., GERSUK, V., SHALEK, A. K., SLICHTER, C. K., MILLER, H. W., MCELRATH, M. J., PRLIC, M., LINSLEY, P. S. and GOTTARDO, R. (2015). MAST: a flexible statistical framework for assessing transcriptional changes and characterizing heterogeneity in single-cell RNA sequencing data. *Genome Biology* **16** 278. .

KAUFMAN, L. and ROUSSEEUW, P. (1987). *Clustering by means of medoids*. North-Holland.

KIM, T., CHEN, I. R., LIN, Y., WANG, A. Y.-Y., YANG, J. Y. H. and YANG, P. (2018). Impact of similarity metrics on single-cell RNA-seq data clustering. *Briefings in Bioinformatics* bby076.

KISELEV, V. Y., KIRSCHNER, K., SCHAUB, M. T., ANDREWS, T., YIU, A., CHANDRA, T., NATARAJAN, K. N., REIK, W., BARAHONA, M., GREEN, A. R. and HEMBERG, M. (2017). SC3: consensus clustering of single-cell RNA-seq data. *Nature Methods* **14** 483 EP -.

KORTHAUER, K. D., CHU, L.-F., NEWTON, M. A., LI, Y., THOMSON, J., STEWART, R. and KENDZIORSKI, C. (2016). A statistical approach for identifying differential distributions in single-cell RNA-seq experiments. *Genome Biology* **17** 222. .

LENG, N., DAWSON, J. A., THOMSON, J. A., RUOTTI, V., RISSMAN, A. I., SMITS, B. M. G., HAAG, J. D., GOULD, M. N., STEWART, R. M. and KENDZIORSKI, C. (2013). EBSeq: an empirical Bayes hierarchical model for inference in RNA-seq experiments. *Bioinformatics* **29** 1035-1043.

LI, F. and ALTIERI, D. C. (1999). The Cancer Antiapoptosis Mouse Survivin Gene. *Cancer Research* **59** 3143.

LIN, P., TROUP, M. and HO, J. W. K. (2017). CIDR: Ultrafast and accurate clustering through imputation for single-cell RNA-seq data. *Genome Biology* **18** 59. .

LOVE, M. I., HUBER, W. and ANDERS, S. (2014). Moderated estimation of fold change and dispersion for RNA-seq data with DESeq2. *Genome Biology* **15** 550. .

MARIONI, J. C. and ARENDT, D. (2017). How Single-Cell Genomics Is Changing Evolutionary and Developmental Biology. *Annual Review of Cell and Developmental Biology* **33** 537-553. PMID: 28813177.

NAVIN, N. E. (2015). The first five years of single-cell cancer genomics and beyond. *Genome Research* **25** 1499–1507.

NAWY, T. (2013). Single-cell sequencing. *Nature Methods* **11** 18 EP -.

PAPALEXI, E. and SATIJA, R. (2017). Single-cell RNA sequencing to explore immune cell heterogeneity. *Nature Reviews Immunology* **18** 35 EP -.

PIERSON, E. and YAU, C. (2015). ZIFA: Dimensionality reduction for zero-inflated single-cell gene expression analysis. *Genome Biology* **16** 241. .

RAY, S. and TURI, R. H. (2000). Determination of Number of Clusters in K-Means Clustering and Application in Colour Image Segmentation.

SOHR, S. and ENGELAND, K. (2008). RHAMM is differentially expressed in the cell cycle and downregulated by the tumor suppressor p53. *Cell Cycle* **7** 3448–3460.

SONESON, C. and ROBINSON, M. D. (2017). Bias, Robustness And Scalability In Differential

Expression Analysis Of Single-Cell RNA-Seq Data. *bioRxiv*.

STREHL, A. and GHOSH, J. (2003). Cluster Ensembles — a Knowledge Reuse Framework for Combining Multiple Partitions. *J. Mach. Learn. Res.* **3** 583–617.

WAGNER, U. and TAUDES, A. (1986). A Multivariate Polya Model of Brand Choice and Purchase Incidence. *Marketing Science* **5** 219–244.

YAKOWITZ, S. J. and SPRAGINS, J. D. (1968). On the Identifiability of Finite Mixtures. **39** 209–214.

ZAPPIA, L., PHIPSON, B. and OSHLACK, A. (2017). Splatter: simulation of single-cell RNA sequencing data. *Genome Biology* **18** 174. .

Appendix.

Proof of Theorem 1. If $\theta \in \bigcup_{\pi \in \Pi} \left[A_\pi \cap M_{g,\pi} \right]$, then there exists a partition π for which $\theta \in A_\pi$ and $\theta \in M_{g,\pi}$. By construction

$$f_g^1(x) = \sum_{k=1}^{K} \phi_k f_{g,k}(x) = \sum_{b \in \pi} \sum_{k \in b} \phi_k f_{g,k}(x) = \sum_{b \in \pi} \Phi_b f_{g,k^*(b)}(x),$$

where $k^*(b)$ indexes any component in b, since all components in that block have the same component distribution owing to constraint $M_{g,\pi}$. Continuing, using the constraint $\theta \in A_\pi$,

$$f_g^1(x) = \sum_{b \in \pi} \Psi_b f_{g,k^*(b)}(x) = f_g^2(x) \qquad \forall x.$$

That is, $\theta \in \text{ED}_g$.

If $\theta \in \text{ED}_g$, then $f_g^1(x) = f_g^2(x)$ for all x. Noting that both are mixtures over the same set of components $\{f_{g,k}\}$, let $\{h_{g,l} : l = 1, 2, \cdots, L\}$ be the set of distinct components over this set, and so

$$f_g^1(x) = \sum_{k=1}^{k} \phi_k f_{g,k}(x) = \sum_{l=1}^{L} c_{g,l}(\phi) h_{g,l}(x) = \sum_{l=1}^{L} c_{g,l}(\psi) h_{g,l}(x) = f_g^2(x)$$

where

$$(11) \quad c_{g,l}(\phi) = \sum_{k=1}^{K} \phi_k 1[f_{g,k} = h_{g,l}] \qquad c_{g,l}(\psi) = \sum_{k=1}^{K} \psi_k 1[f_{g,k} = h_{g,l}].$$

Finite mixtures of distinct negative binomial components are identifiable (Proposition 5 from Yakowitz and Spragins (1968)), and so the equality of f_g^1 and f_g^2 implies $c_{g,l}(\phi) = c_{g,l}(\psi)$ for all $l = 1, 2, \cdots, L$. Identifying the partition blocks $b_l = \{k : f_{g,k} = h_{g,l}\}$, and the partition $\tilde{\pi} = \{b_l\}$, we find $\theta \in A_{\tilde{\pi}} \cap M_{g,\tilde{\pi}}$. The accumulated probabilities in (11) correspond to $\Phi_{\tilde{\pi}}$ and $\Psi_{\tilde{\pi}}$, which are equal on $A_{\tilde{\pi}}$.

Pseudo-code.
ADDRESS OF THE FIRST AND SECOND AUTHORS
USUALLY A FEW LINES LONG
E-MAIL: ma79@wisc.edu
    kendzior@biostat.wisc.edu

ADDRESS OF THE THIRD AUTHOR
USUALLY A FEW LINES LONG
USUALLY A FEW LINES LONG
E-MAIL: newton@stat.wisc.edu
URL: http://www.foo.com

Algorithm 2 scDDboost

    Input:

        genes by cells expression data matrix $X = (X_{g,c})$

        cell condition labels $y = (y_c)$

        number of cell subtypes K

        number of randomized clusterings n_r

    Output: posterior probabilities of differential distribution

    procedure scDDboost(X, y, K, n_r)

2:      distance matrix: $D = \mathrm{dist}(X) \leftarrow$ pairwise distances between cells (columns of X)

        hyper-parameters $(\hat{a}, \hat{b}) \leftarrow \mathrm{hyper}(D)$

4:     **repeat**

          Gamma noise vector: e, with components $\sim \mathrm{Gamma}(\hat{a}, \hat{b})$

6:        randomized distance matrix: $D^* \leftarrow D/(e\mathbf{1}^T + \mathbf{1}e^T)$

          $\hat{z}^* \leftarrow K-\mathrm{medoids}(D^*)$

8:        $P^* \leftarrow$ scDDboost-core$(X, y, \hat{z}^*)$

        until n_r randomized distance matrices

10:    **return** $\forall$ genes g, $P(\mathrm{DD}_g|X, y) = \frac{1}{n_r} \sum_{D^*} P_g^*$

    end procedure